THE JOURNAL OF PHYSICAL CHEMISTRY B

Article

pubs.acs.org/JPCB

Quantitative Evaluation of Adhesion of Osteosarcoma Cells to Hydrophobic Polymer Substrate with Tunable Elasticity

Hiroshi Y. Yoshikawa,[†,‡] Jing Cui,[§] Karl Kratz,[§] Takahisa Matsuzaki,[‡] Seiichiro Nakabayashi,[‡] Astrid Marx,[∥] Ulrike Engel,[∥] Andreas Lendlein,*[,§] and Motomu Tanaka*[,⊥]

[†]Physical Chemistry of Biosystems, Institute of Physical Chemistry, University of Heidelberg, 69120 Heidelberg, Germany

[‡]Department of Chemistry, Saitama University, 338-8570 Saitama, Japan

[§]Centre for Biomaterial Development and Berlin-Brandenburg Center for Regenerative Therapies, Institute of Polymer Research, Helmholtz-Zentrum Geesthacht, 14513 Teltow, Germany

[∥]Nikon Imaging Center at the University of Heidelberg, BIOQUANT, 69120 Heidelberg, Germany

[⊥]Cell Biophysics Group, Institute for Toxicology and Genetics, Karlsruhe Institute of Technology, 76131 Karlsruhe, Germany

Supporting Information

ABSTRACT: We investigated a potential application of hydrophobic poly(*n*-butyl acrylate) networks (cP*n*BA) as substrates with tunable elasticity for culturing, maintenance, and regulation of human osteosarcoma cells (U2OS). Nanoindentation experiments with an atomic force microscope revealed that the mechanical properties of cP*n*BA films are maintained under aqueous conditions, confirming that the substrate elasticity can be controlled simply by the degree of cross-linking, independent from the culture medium. We found that the adhesion U2OS cells to cP*n*BA substrates could be improved by surface treatments such as oxgen plasma and serum proteins. To determine the strength of cell adhesion, the critical pressure to detach cells from cP*n*BA substrates was measured using a shock wave induced by an intensive picosecond laser pulse. A monotonic increase in the cell adhesion strength in accordance with the substrate elasticity demonstrated the potential of intrinsically hydrophobic cP*n*BA as a new class of substrate material with tunable mechanical properties that are not influenced by the culture medium.

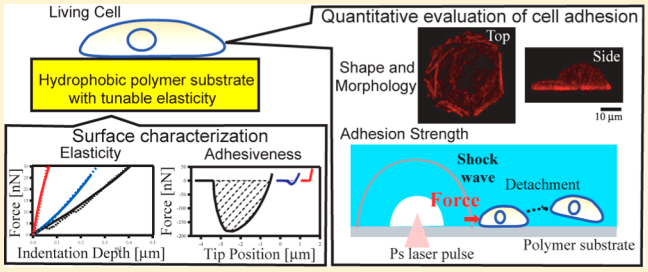

INTRODUCTION

In recent years, an increasing number of studies have provided compelling evidence that biological cells have the capability of sensitively responding not only to their biochemical environment but also to their mechanical environment (so-called mechanosensing).[1] Using chemically cross-linked hydrogels as a model for soft extracellular matrix (ECM) surfaces, it has been demonstrated that the mechanical properties (Young's modulus, E) of substrates play crucial roles in various cellular processes such as morphology and motility of contractile cells[2−6] and differentiation of mesenchymal stem cells (MSCs).[7,8] So far, various hydrogels such as polyacrylamide and hyaluronic acid have been widely used to model soft micromechanical environments like brain tissue ($E \sim 1$ kPa) and muscle tissue ($E \sim 10$ kPa).[7,9,10] As an alternative to hydrogels, hydrophobic polymers like poly(dimethylsiloxane) segments (PDMS) would offer advantages in fine-tuning of a stiffer region from 10 kPa to 1 MPa,[11] which are comparable to relatively stiff tissues like premineralized collagenous bone ($E \geq 30$ kPa) and blood vessels ($E \geq 100$ kPa).[7,12] However, pure PDMS was reported to be cytotoxic for mesenchymal stem cells.[13]

In the previous accounts, Cui et al. examined the practical use of amorphous, hydrophobic poly(*n*-butyl acrylate) networks (cP*n*BA) as a candidate of polymetric biomaterials with adjustable mechanical properties.[14] cP*n*BAs were synthesized via bulk radical polymerization from *n*-butyl acrylate (*n*BA) and a low molecular weight poly(propylene glycol) dimethacrylate (PPGDMA, $M_n = 560$ g mol^{-1}) as cross-linker. The tensile tests demonstrated that the bulk elastic modulus of cP*n*BAs at room temperature could systematically be adjusted from 100 kPa to 10 MPa by increasing the cross-linker concentration, while the glass transition temperature (T_g) was found to increase from −46 to −22 °C.

Previous cytotoxicity tests with fibroblasts (L929 mouse fibroblasts)[14] and primary endothelial cells (HUVEC)[15] revealed that the cP*n*BA samples showed no cytotoxic effects and did not influence the integrity of membrane and mitochondrial activity of HUVEC. cP*n*BA samples exhibited a low endotoxin content below the 0.5 EU/mL limit of the Food and Drug Administration and did not activate the innate immune system.[16,17] The following hemocompatibility tests suggested a moderate thrombogenicity of cP*n*BA, suggesting that the optimization of surface functionalization would be necessary for the applications in cardiovascular tissue engineering.[18] Last but not

Received: December 22, 2011
Revised: May 2, 2012
Published: June 20, 2012

   dx.doi.org/10.1021/jp212385p | *J. Phys. Chem. B* 2012, 116, 8024−8030

least, HUVEC showed poorer adhesion and less actin stress fiber formation on cP*n*BA substrates that possess ~2 orders of magnitude higher elastic modulus, suggesting the importance of mechano-compliance between cells and contact substrates.[15]

In this work, the mechano-response of cells on substrates based on hydrophobic polymers was investigated by systematically evaluating the surface properties of cP*n*BA films and their impact on cell adhesion. The mechanical and adhesive properties of cP*n*BA films were carefully evaluated by nanoindentation with an atomic force microscope (AFM). On the basis of the range of the determined film elasticities, we selected human osteosarcoma cells (U2OS) for the evaluation of their adhesion, since their contact tissues possess comparable elasticity to the cP*n*BA films.[7] Adhesion of U2OS cells to cP*n*BA with different surface treatments was investigated. Cell shape was evaluated with bright-field and fluorescence microscopy. In addition, the adhesion strength between U2OS cells and cP*n*BA substrate was quantitatively evaluated by the picoseond laser-induced cell detachment assay,[19] where the critical detachment pressure for the cell detachment can be determined by picosecond laser-induced pressure waves.

EXPERIMENTAL SECTION

Materials. Deionized water from a Milli-Q device (Millipore, Molsheim, France) was used throughout this study. Unless stated otherwise, all other chemicals were purchased either from Sigma-Aldrich (Munich, Germany) or Carl Roth (Karlsruhe, Germany) and were used without further purification.

Synthesis and Preparation of cPnBA Films. cP*n*BA polymer networks with various content (S1: 0.44 wt %; S2: 2.14 wt %; S3: 7.34%; S4: 25.93 wt %; and S5: 41.18 wt %) of poly(propylene glycol) dimethacrylate (PPGDMA, M_n = 560 g mol^{-1}) as cross-linker was synthesized by thermally induced free radical polymerization, as reported in our previous paper.[14] cP*n*BA substrates with a diameter of 13 mm and a thickness of 1 mm were punched out of the obtained cP*n*BA films and purified as described in the previous report.[14]

Plasma Treatment of cPnBA Substrates. Oxygen plasma treatment of cP*n*BA samples was performed in a tubular microwave-plasma reactor system operating at 2.45 GHz (modified Plaslan 500, JE PlasmaConsult, Wuppertal, Germany). The reactor consisted of a quartz bell jar (diameter: 16 cm; height: 50 cm) mounted on the reactor chamber (diameter and height of 50 cm). The microwave power was coupled to the reactor by an angular slot antenna. The cP*n*BA samples were fixed 7 cm downstream the glow discharge region for treatment with oxygen gas. After the samples were placed into the reactor the system was evacuated to a pressure of 10^{-3} mbar for 10 min and purged with oxygen for 10 min. At a process pressure of 0.5 mbar the oxygen plasma was ignited, and cP*n*BA specimens were treated for 120 s at 1000 W.

Sterilization of cPnBA Substrates. 2D cP*n*BA test specimens were sterilized by gas sterilization using ethylene oxide (EtO; gas phase: 10% EtO, 548C, 65% relative humidity, 1.7 bar, gas exposure time 3 h, aeration phase 21 h) as described in the previous report.[14]

Contact Angle Measurements. The dynamic contact angle (DCA) of the sterilized plain and surface-treated cP*n*BA test specimens was analyzed using captive bubble method on a DSA 100 (KRŰSS, Hamburg, Germany) at ambient temperature according to a previously reported method,[15] whereby prior to the DCA measurement all samples were preconditioned for 1 h in deionized water at ambient temperature for equilibration.

Nanoindentation of cPnBA Films. Nanoindentation of cP*n*BA films was performed using an atomic force microscope (NanoWizard, JPK instruments, Berlin, Germany). Commercial silicon cantilevers with spring constant k = 0.03 N/m or 1.75 N/m with a conical tip (Mikromash, Tallinn, Estonia) were used. Force−indentation (f−i) curves of cP*n*BA films were obtained in the atmosphere or in a 10 mM phosphate buffered saline (PBS) solution (pH 7.4). The apparent Young's modulus, E, of cP*n*BA films were calculated from the approach curves using Sneddon's modification of the Hertz model.[20,21]

$$F = \frac{2\tan(\alpha)}{\pi}\frac{E}{1-\mu^2}\delta^2 \quad (1)$$

where F is the load, δ the indentation depth, μ the Poisson ratio, and α a semivertical angle of the indenter. In this study, μ and α were assumed to be 0.45 and 20°, respectively. Pull-off force, $F_{\text{pull-off}}$, and work of adhesion, U_{ad} (integration of adhesion load ($F \leq 0$), with tip displacement), were obtained from the retraction curves with the maximum load force of 40 nN.

Surface Pretreatment. The plasma-treated substrates were immersed overnight in a PBS buffer at ambient temperature prior to cell culture, while for the pretreatment by serum, cP*n*BA films were immersed overnight in a PBS buffer solution and subsequently overnight in a L15 medium (Gibco, Germany) supplemented with 10% fetal bovine serum (FBS).

Adsorption of Serum Proteins. cP*n*BA substrates were immersed in the PBS buffer (pH 7.4) containing 2.5 mg/mL of fluorescently labeled bovine serum albumin (FITC-BSA, Sigma-Aldrich) for 30 min. The fluorescence intensity near the film surface was observed in the PBS buffer (no BSA) using an inverted microscope (TE-2000U, Nikon Instruments Inc.) coupled to a CCD camera (C-4742-95, Hamamatsu Photonics). The amounts of FITC-BSA adsorbed to cP*n*BA substrates were estimated by the calibration with the fluorescence intensity of a known amount of FITC-BSA adsorbed on a polystyrene bead.[22] We first incubated FITC-BSA solutions with 2 μm polystyrene beads (0.05 g/mL) and measured the difference between the initial and the residual FITC-BSA concentrations in the supernatant. The concentration of FITC-BSA was determined by measuring absorbance using a calibration curve obtained first at a wavelength of 280 nm. After the equilibrium was reached, the equation

$$\Gamma = \nu\left[\frac{C_i - C_f}{m\Sigma}\right] \quad (2)$$

where ν (m^3) is the volume of the solution, C_i (g/m^3) and C_f (g/m^3) are the initial and final concentrations of the adsorbate in solution, m (g) is the mass of the adsorbent, and Σ (m^2/g) is the specific area of the adsorbent.[22] The prepared beads were resuspended in a PBS buffer solution, and their fluorescence intensity was measured by the same microscope to quantify the amount of FITC-BSA per particle, which yields the relationship between FITC-BSA and fluorescence intensity.

Cell Culture. Human osteosarcoma cells (U2OS cells) expressing TagRFP-labeled β-actin (Marinpharm GmbH, Luckenwalde, Germany) were maintained in polystyrene flasks in a 5% CO_2 incubator at 37 °C and cultured in Dulbelcco's modified Eagle's medium (Gibco, Germany) supplemented with 10% fetal bovine serum (FBS), 2 mM L-alanyl-L-glutamine, 1% nonessential amino acids, 20 U/mL penicillin, and 100 μg/μL streptomycin (PAA Laboratories, Cölbe, Germany). For the cell

dx.doi.org/10.1021/jp212385p | J. Phys. Chem. B 2012, 116, 8024−8030

adhesion experiments, U2OS cells with a number density of 20 cells/mm^2 were seeded on cP*n*BA films in a plastic Petri dish and cultured with a L15 medium (Gibco, Germany).

Area and Shape Analysis of Cells. The adhesion behavior of cells on cP*n*BA films was monitored using an inverted microscope (TE-2000U, Nikon Instruments Inc.) with a cooled CCD camera (Hamamatsu, Japan). The projected area and elongation (the ratio between minor and major axis) of the adherent cells were calculated using image analysis software, ImageJ. For confocal fluorescence microscopy, U2OS cells cultured for 3 h culture on cP*n*BA films were fixed with 4% formaldehyde for 20 min at room temperature. The samples were mounted onto coverslips in PBS and viewed with a laser-scanning confocal microscope (A1R, Nikon Instruments Inc.) with a 60× objective (N.A. = 1.2, water immersion, Nikon Instruments Inc.). The resulting confocal images were deconvolved using Huygens deconvolution software (Scientific Volume Imaging, Netherlands).

Picosecond Laser Cell Detachment Assay. The experimental system for the measurement of cell adhesion strength by picosecond laser-induced shock wave was described in our previous report.[19] A picosecond Nd:YAG laser system (λ = 1064 nm, τ = 60 ps, PY 61C-20, Continuum, Santa Clara, CA) was used to induce shock waves. The picosecond laser pulses were led through an inverted microscope and focused through a 20× objective lens (N.A. = 0.75, Nikon Instruments Inc.). A single picosecond laser pulse was focused into a culture medium at a fixed distance of 2 mm from cells and 100 μm above a cP*n*BA film surface. The laser energy was adjusted with a polarizer and measured with a power meter (PE 10-S, OPHIR). The minimum energy needed to detach cells from substrate is defined as the critical detachment energy. This parameter was determined by systematically varying the detachment energy until the minimum threshold value was achieved for cell detachment from the substrate. The corresponding critical pressure (i.e., the minimum pressure required for cell detachment) was then calculated from the energy−pressure curve obtained in water using a factory-calibrated pressure sensor (Müller-Platte Needleprobe, Müller Instruments, Oberursel, Germany).

RESULTS AND DISCUSSION

Elastic and Adhesive Properties of cPnBA Films. Figure 1 shows the force−indentation (f−i) curves (approach) of cP*n*BA films with different cross-linker content in air and in a PBS solution. The f−i curves between air and PBS are almost identical for all investigated cP*n*BA films. The apparent Young's modulus, E, of cP*n*BA films were calculated from the f−i curves using the modified Hertz model, which assumes the contact between a cone with infinitely small apex and a flat surface. Here, the influence of the indentation depth on the calculated apparent elastic modulus was carefully optimized by changing the fitting regions until one can achieve self-consistent values (see Supporting Information). The apparent Young's modulus in air increased significantly from E(S1) = 130 kPa to E(S5) = 7.0 MPa with rising cross-linker content (in Table 1), showing good agreement with values previously measured by a tensile tester.[14] It should be noted that difference in E between air and PBS is less than 10%. Figure 2 shows the retract curves of cP*n*BA films in air. The pull-off force, $F_{\text{pull-off}}$, decreased from $F_{\text{pull-off}}$(S1) = 180 nN to $F_{\text{pull-off}}$(S5) = 10 nN according to the increase in the E values. The work of adhesion, U_{ad}, was also increased from 0.8 to 370 fJ, accordingly. On the other hand, the pull-off force and work of adhesion became drastically small ($F_{\text{pull-off}}$ < 5 nN, U_{ad} < 1 fJ) in PBS solutions.

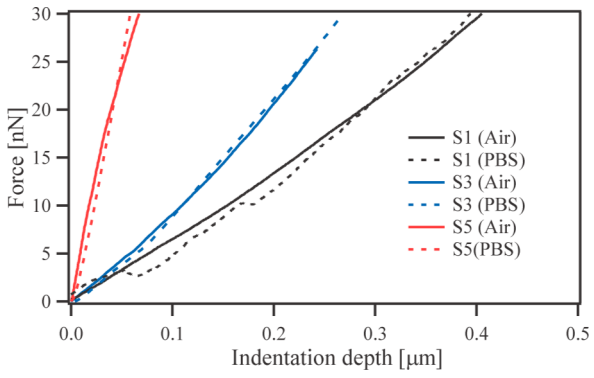

Figure 1. Force−indentation (f−i) curves of cP*n*BA films of S1, S3, and S5 in air (solid line) and in PBS buffers (dashed line) recorded at 25 °C.

The similar E values achieved in air and PBS suggest that no swelling of cP*n*BA films occurs even in a nanoscale. The hydrophobicity of cP*n*BA films can guarantee the precise tuning of the substrate elasticity under physiological conditions with various ionic strength or pH value. The adhesiveness of the cP*n*BA films is attributed to the density of flexible P*n*BA chains and compliant backing. Sitti et al. systematically investigated the adhesiveness of layers of P*n*BA dangling chains grafted on a bulk elastomer (PDMS) surface by AFM and found that the dangling chains are fully extended as the AFM tip retracts, leading to an increase in the amount of work adhesion.[23] For the investigated cP*n*BA films, we assume an increase in the number-average molecular weight of each flexible P*n*BA chain with decreasing cross-linker density, which should result in a thicker and dense layer of flexible P*n*BA chains on the substrate surface. Such dense layers of flexible chains on a backing should exhibit a high adhesiveness, which is reasonable for our AFM results. In addition, the reduction of the adhesiveness is also due to the influence of the media between a Si tip and a cP*n*BA film; the smaller contributions to dispersion and/or dipole−dipole interactions in water (n = 1.33, ε = 80) than in air (n = 1, ε = 1).

Influence of Surface Treatments on Cell Adhesion to cPnBA Films. Figure 3A shows representative confocal fluorescence images of U2OS cells cultured for 3 h on S1 films (E = 130 kPa) with different surface treatments. Although no U2OS cells adhered to bare, nontreated cP*n*BA films (adherent cells are less than 1% of total seeded cells), they adhered to the cP*n*BA films treated either with serum or O_2 plasma. The three-dimensional visualization of RFP-actin reveals that more pronounced stress fiber formation and flattening of U2OS cells occur on serum-treated films, while cells adopt a hemispherical shape on films treated with O_2 plasma. Cell adhesion to the two different surfaces was also statistically investigated by projected area (Figure 3B) and cell density (Figure 3C). The projected area of cells shows the significant difference between two treatments: 1300 ± 480 μm^2 (serum-treated) and 587 ± 209 μm^2 (O_2 plasma-treated). On the other hand, cell densities for the two surfaces are comparable (~1000 cells/mm^2).

Previously, Lee et al. systematically studied the influence of the surface functional group of polymer substrate on adhesion of Chinese hamster ovary cells. They found that cell adhesion, spreading, and growth properties were significantly facilitated on the surfaces with high hydroxyl group density achieved by

dx.doi.org/10.1021/jp212385p | J. Phys. Chem. B 2012, 116, 8024−8030

Table 1. Mechanical and Adhesive Properties of Poly(*n*-butyl acrylate) Networks with Different Contents of Cross-Linker, Poly(propylene glycol) Dimethacrylate (PPGDMA, M_n = 560 g mol^{-1})

sample ID	PPGDMA [wt %]	E_{air} [MPa]	E_{PBS} [MPa]	E_{PBS}/E_{air}	$F_{pull\text{-}off}$ (air) [nN]	$F_{pull\text{-}off}$ (PBS) [nN]	U_{ad} (air) [fJ]	U_{ad} (PBS) [fJ]
S1	0.44	0.13 ± 0.01	0.12 ± 0.01	0.92	181.7 ± 12.8	4.3 ± 1.7	371.2 ± 37.7	1.3 ± 0.6
S2	2.14	0.33 ± 0.01	0.31 ± 0.11	0.93	35.9 ± 2.2	1.4 ± 0.7	25.9 ± 3.5	0.1 ± 0.1
S3	7.34	0.94 ± 0.09	0.93 ± 0.14	0.99	13.3 ± 0.6	0.3 ± 0.2	3.2 ± 0.3	0.0
S4	25.93	4.28 ± 0.13	4.04 ± 1.23	0.94	7.6 ± 0.6	0.1 ± 0.1	0.5 ± 0.1	0.0
S5	41.18	7.05 ± 1.16	6.35 ± 1.65	0.90	11.3 ± 2.2	0.1 ± 0.1	0.8 ± 0.1	0.0

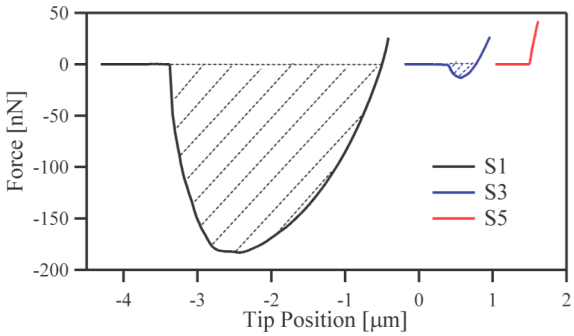

Figure 2. Force−distance curves (retraction) of S1, S3, and S5 in air at 25 °C measured during the retraction from the surface. Preload for all samples were set to be 40 nN. Work of adhesion, *U*, was estimated from the integration of the dotted region under 0 N.

water vapor plasma treatments.[24,25] In fact, as reported by Bell and Dembo, cell adhesion can physically be described as the wetting of surfaces.[26,27] Thus, it is plausible that the surface tension significantly influences cell adhesion, although the adhesion of cells are not only governed by the tension (plastic deformation) but also determined by the elasticity of cells.[28,29] To examine if the cell spreading on substrates depends on the hydrophilicity of cP*n*BA films, we measured the dynamic contact angles (advancing and receding contact angles) with air bubbles in a PBS buffer. As summarized in Table 2, O_2 plasma treatment of S1 substrates leads to a clear decrease in the advancing contact angle from 123 ± 4° to 89 ± 9°, which can be attributed to the formation of carbonyl groups with a peroxide-like structure on the polymer surface, as previously reported for O_2 plasma-treated poly(*n*-butyl acrylate).[30] O_2 plasma treatment also decreased advancing contact angle of cP*n*BA substrates with different stiffness, e.g., S3: 111 ± 4° to 86 ± 5°. The serum treatment also decreased the contact angle to a similar value, $\theta_{advancing}$ = 89 ± 4° (S1), due to the nonspecific adsorption of serum proteins onto the surface. To discriminate the influence of O_2 plasma and serum treatments, we evaluated the adsorption of BSA, which is one of the major serum proteins in our medium. Figure 4 represents the fluorescence intensities of FITC-BSA for the substrates with and without O_2 plasma treatments, measured for S1 and S3. For both samples, we found that the hydrophilic treatments by O_2 plasma results in a significant decrease in the adsorption of BSA, which is consistent with previous reports on gold and polymer substrates.[31,32] In addition, the adsorbed amounts (200−400 ng/cm^2) are reasonable for the amounts of BSA adsorbed to hydrophobic polymer substrate.[31−33]

It should be noted that the more pronounced cell adhesion was found on serum-treated substrates than on the film treated with O_2 plasma (Figure 3), although there was no significant difference in hydrophilicity. Rather, it can be explained by the adsorption of serum proteins such as fibronectin, which is specifically recognized by integrin receptors. In fact, the influence of serum proteins on the

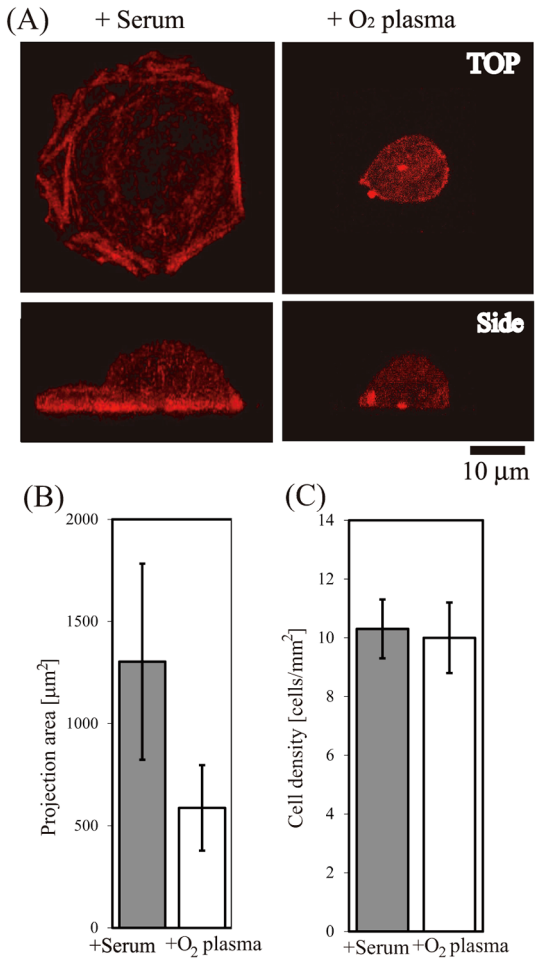

Figure 3. (A) Confocal fluorescence images, (B) projected area, and (C) cell density of U2OS cells after 3 h on S1 substrate (E = 120 kPa) treated with serum or O_2 plasma. The confocal fluorescence images represent maximal projection along the optical axis (z-axis, top) and a side projection (y-axis, side). The error bars in (B) and (C) represent standard deviations (n = 100).

Table 2. Summary of Dynamic Contact Angle Measurements of cP*n*BA Films (S1, E = 120 kPa) with Different Pretreatments

surface treatment	θ advancing [deg]	θ receding [deg]	θ hysteresis [deg]
−serum, −O_2 plasma	122.6 ± 3.8	33.3 ± 3.4	89.3
−serum, +O_2 plasma	88.6 ± 9.0	23.9 ± 1.4	64.7
+serum, −O_2 plasma	88.5 ± 4.1	22 4 ± 2.3	66.1
+serum, +O_2 plasma	87.8 ± 3.8	21.0 ± 1.4	66.8

dx.doi.org/10.1021/jp212385p | J. Phys. Chem. B 2012, 116, 8024−8030

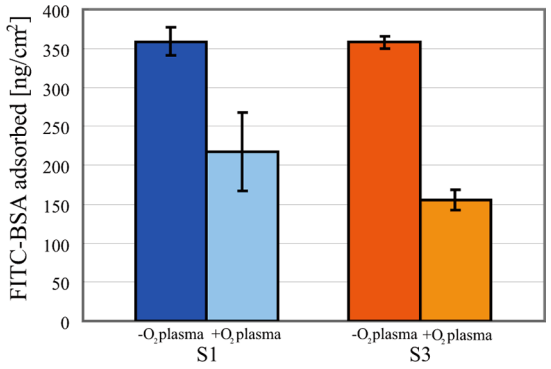

Figure 4. Amounts of FITC-BSA adsorbed on the cP*n*BA films (S1 and S3) with and without O_2 plasma treatments. The error bars represent standard deviations (n = 10).

surface seems to play dominant roles, as the projected area of U2OS cells on serum-treated substrates showed a slight increase when they are pretreated with O_2 plasma (1860 ± 810 μm^2).

Impact of cPnBA Film Stiffness on Cell Adhesion. In the next step, we investigated the adhesion of U2OS cells on soft S1 (E = 120 kPa) and stiff S3 (E = 930 kPa) samples and analyzed the adhesion behavior in terms of cell shape and cell adhesion strength. In order to highlight the influence of substrate elasticity, we used the serum-treated cP*n*BA films without the O_2 plasma treatment that showed comparable surface adsorption of serum proteins (Figure 4). Figure 5 shows representative (A) epifluorescence and (B) confocal fluorescence images of U2OS cells at t = 3 h and t = 48 h. We found that the formation of spreading front and stress fibers was more pronounced on stiffer S3 substrates than on softer S1 substrates at t = 3 h. Although single U2OS cells on S1 and S3 substrates were flattened and exhibited pronounced stress fiber formation at t = 48 h, we found that the surface of confluent U2OS layers on stiffer substrates (S3 and S5) was much smoother than that of U2OS cells on softer S1 substrates (Figure 6). Figure 7

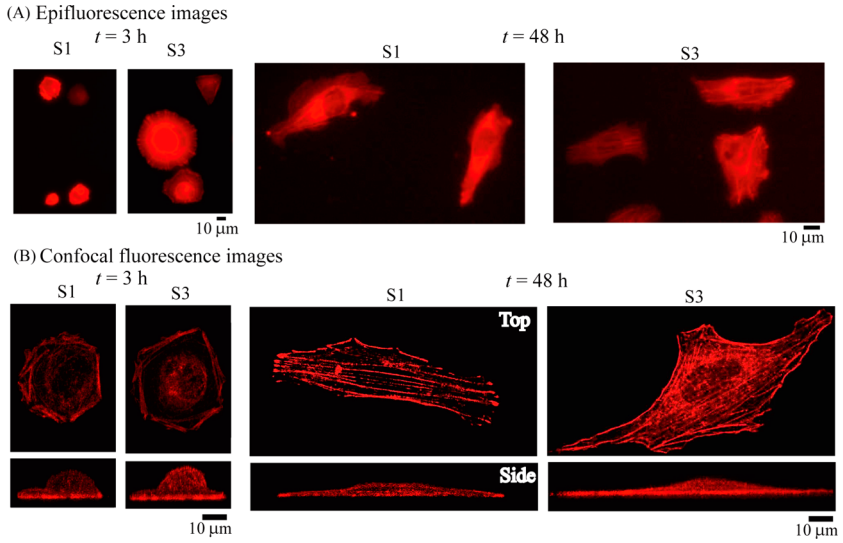

Figure 5. Representative (A) epifluorescence and (B) confocal fluorescence images of U2OS cells on S1 (E = 120 kPa) or S3 (E = 930 kPa) substrates treated with serum. The U2OS cells were fixed at t = 3 h and t = 48 h. The confocal fluorescence images represent maximal projection along the optical axis (z-axis, top) and a side projection (y-axis, side).

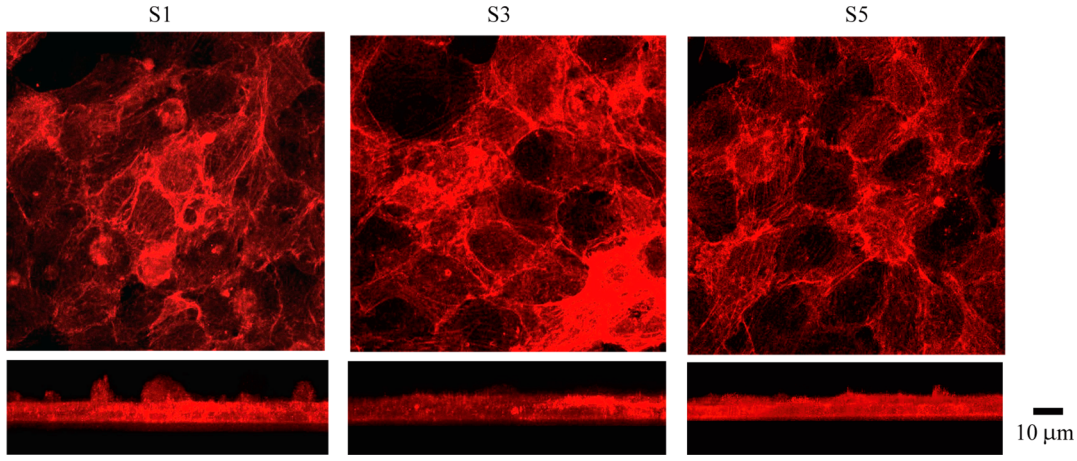

Figure 6. Representative confocal fluorescence images of U2OS cell sheets on S1 (E = 120 kPa), S3 (E = 930 kPa), or S5 (E = 6.36 MPa) substrates treated with serum. To achieve confluent cell layers, cells were placed at a high surface density (5×10^2 cells/mm^2) on the substrate, and the cells were cultured for 48 h. The confocal fluorescence images represent maximal projection along the optical axis (z-axis, top) and a side projection (y-axis, side).

dx.doi.org/10.1021/jp212385p | J. Phys. Chem. B 2012, 116, 8024–8030

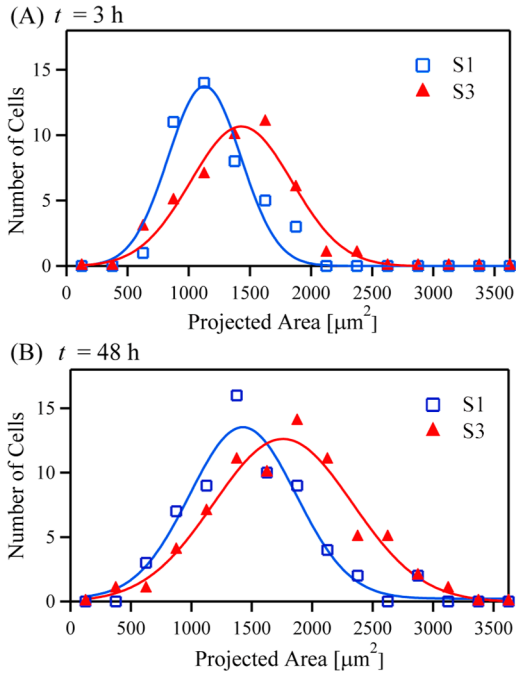

Figure 7. Histograms of projected area of U2OS cells on S1 (E = 120 kPa) or S3 (E = 930 kPa) substrates treated with serum at (A) t = 3 h and (B) t = 48 h. The solid lines represent fitting curves with Gaussian functions.

shows histograms of the projected area of U2OS cells at (A) t = 3 h and (B) t = 48 h, respectively. The histograms can be well-fitted with single Gaussian functions, confirming the statistical reliability. It should be noted that the peak positions reflect the substrate elasticity. At t = 3 h (panel A), the projected area on S1 takes its maximum at A_{S1} = 1100 μm^2, while the corresponding value on S3 is A_{S3} = 1400 μm^2. The same tendency could be observed at t = 48 h (panel B), A_{S1} = 1400 μm^2 and A_{S3} = 1800 μm^2, respectively. In addition, the average of cell elongation (length/width ratio of a cell defined within a minimum bounding box) is increased from 1.36 to 1.50 (3 h) and 2.85 to 3.57 (48 h) according to the increase in stiffness, which is a typical mechano-response of contractile cells.[2−4]

To evaluate the strength of cell adhesion on these synthetic cP*n*BA films, we utilized pressure waves induced by picosecond laser pulses (Figure 8A).[19] This assay enables one to determine the critical pressure, P_{th}, required to cause the detachment of adherent cells in a quantitative manner without damaging cells.

As presented in Figure 8B, the critical pressure for the detachment of U2OS cells after 1 h culture was P_{th} = 7.4 ± 1.6 MPa on soft S1 samples. On stiff S3 samples, P_{th} showed a distinct increase to P_{th} = 8.8 ± 1.3 MPa. The obtained results demonstrated that the careful optimization of surface pretreatments of intrinsically hydrophobic cP*n*BA would enable one to use them as substrate materials for not only culturing but also controlling the adhesion of bone cells.

CONCLUSIONS

In this article, we investigated a potential application of non-swelling hydrophobic poly(*n*-butyl acrylate) networks (cP*n*BA) as substrates with tunable elasticity in culturing, maintenance, and regulation of human osteosarcoma cells (U2OS). Nanoindentation experiments with AFM revealed that the mechanical properties of cP*n*BA films are maintained under aqueous conditions, confirming that the substrate elasticity can be controlled simply by the degree of cross-linking, independent from the culture medium. We found that U2OS cells do not adhere on the untreated substrates, but cP*n*BA substrates become compatible to U2OS cells by the pretreatments with serum or O_2 plasma. In particular, live cell images and the analysis of cell morphology revealed the stable adhesion and spreading of U2OS cells on the cP*n*BA substrates pretreated with serum. The critical pressure to detach cells from cP*n*BA films could quantitatively be determined using a strong shock wave induced by an intensive picosecond laser pulse, showing a monotonic increase in the cell adhesion strength in accordance with the substrate elasticity. These results clearly indicate the potential of the cP*n*BA films for the detailed investigation of mechano-sensing of contractile cells independent from the composition of culture media (e.g., salt, pH). We believe that surface-treated cP*n*BA films with tunable elasticity will be a useful experimental biomaterial platform to provide insights into the fundamental mechanism of cell mechano-sensing, which can be extended in a next step toward in regenerative medicine.

ASSOCIATED CONTENT

Supporting Information

Dependence of the fitting region on Young's modulus. This material is available free of charge via the Internet at http://pubs.acs.org.

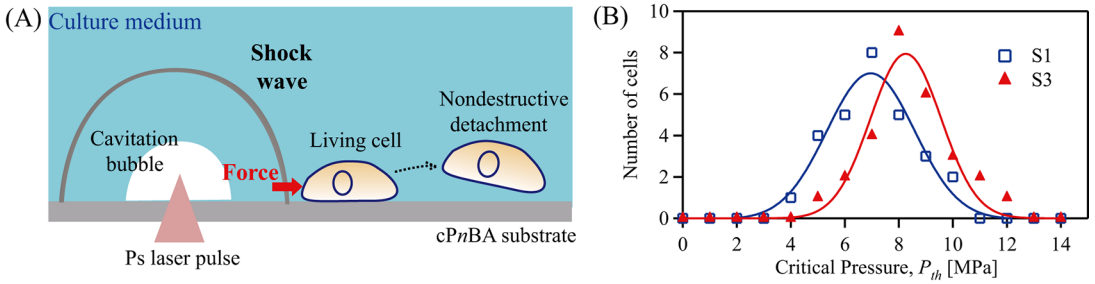

Figure 8. (A) Schematic illustration of nondestructive detachment of cells from cP*n*BA films. Pressures generated by picosecond laser pulses can be calibrated by the pulse energy and the distance between the focal point and the target cell, which enables the cell adhesion strength to be determined quantitatively. (B) Histograms of critical shock wave pressure, P_{th}, required to cause cell detachment from cP*n*BA films of S1 (open square) and S3 (red triangle) with serum treatment. Cells after 1 h culture were detached with picosecond laser-induced shock waves. The solid lines represent fits to the histograms using Gaussian functions.

dx.doi.org/10.1021/jp212385p | J. Phys. Chem. B 2012, 116, 8024−8030

AUTHOR INFORMATION

Corresponding Author

*Tel +49-(0)-6221-544916; Fax +49-(0)-6221-544918; e-mail tanaka@uni-heidelberg.de (M.T.), andreas.lendlein@hzg.de (A.L.).

Notes

The authors declare no competing financial interest.

ACKNOWLEDGMENTS

M.T. and U.E. are the members of the German Excellence Cluster "Cell Network" and BIOQUANT. M.T. is thankful to the Helmholtz Association for support through the "BioInterface" program. H.Y.Y. thanks the Alexander von Humboldt Foundation for a research fellowship and Japan Society for the Promotion of Science for the support by KAKENHI (No. 24656006, 24680050, 24106505, and 23850006). H.Y.Y. and T.M. thank Saitama Univ. for the support through the "Kanryu" exchange program. A.L. is thankful to the Helmholtz Association for support through the "Regenerative Medicine and Active Biomaterials" cross program activity. J.C., K.K., and A.L. thank the Deutsche Forschungsgemeinschaft for the support under grant SFB760, subproject B3. We are grateful to Lydia Haussmann (MarinPharm GmbH) for donation of U2OS cells.

REFERENCES

(1) Discher, D. E.; Janmey, P.; Wang, Y. L. *Science* **2005**, *310*, 1139−1143.
(2) Lo, C. M.; Wang, H. B.; Dembo, M.; Wang, Y. L. *Biophys. J.* **2000**, *79*, 144−152.
(3) Gray, D. S.; Tien, J.; Chen, C. S. *J. Biomed. Mater. Res., Part A* **2003**, *66A*, 605−614.
(4) Engler, A.; Bacakova, L.; Newman, C.; Hategan, A.; Griffin, M.; Discher, D. *Biophys. J.* **2004**, *86*, 617−628.
(5) Kidoaki, A.; Matsuda, T. *J. Biotechnol.* **2008**, *133*, 225−230.
(6) Papenburg, B. J.; Vogelaar, L.; Bolhuis-Versteeg, L. A. M.; Lammertink, R. G. H.; Stamatialis, D.; Wessling, M. *Biomaterials* **2007**, *28*, 1998−2009.
(7) Engler, A. J.; Sen, S.; Sweeney, H. L.; Discher, D. E. *Cell* **2006**, *126*, 677−89.
(8) Discher, D. E.; Mooney, D. J.; Zandstra, P. W. *Science* **2009**, *324*, 1673−7.
(9) Flanagan, L. A.; Ju, Y. E.; Marg, B.; Osterfield, M.; Janmey, P. A. *NeuroReport* **2002**, *13*, 2411−2415.
(10) Engler, A. J.; Griffin, M. A.; Sen, S.; Bonnemann, C. G.; Sweeney, H. L.; Discher, D. E. *J. Cell Biol.* **2004**, *166*, 877−87.
(11) Rehfeldt, F.; Engler, A. J.; Eckhardt, A.; Ahmed, F.; Discher, D. E. *Adv. Drug Delivery Rev.* **2007**, *59*, 1329−39.
(12) Lee, H. Y.; Oh, B. H. *Circ. J.* **2010**, *74*, 2257−62.
(13) Neuss, S.; Apel, C.; Buttler, P.; Denecke, B.; Dhanasingh, A.; Ding, X. L.; Grafahrend, D.; Groger, A.; Hemmrich, K.; Herr, A.; Jahnen-Dechent, W.; Mastitskaya, S.; Perez-Bouza, A.; Rosewick, S.; Salber, J.; Woltje, M.; Zenke, M. *Biomaterials* **2008**, *29*, 302−313.
(14) Cui, J.; Kratz, K.; Hiebl, B.; Jung, F.; Lendlein, A. *Polym. Adv. Technol.* **2011**, *22*, 126−132.
(15) Hiebl, B.; Cui, J.; Kratz, K.; Frank, O.; Schossig, M.; Richau, K.; Lee, S.; Jung, F.; Lendlein, A. *J. Biomater. Sci., Polym. Ed.* **2012**, *23*, 901−915.
(16) Mayer, A.; Kratz, K.; Hiebl, B.; Lendlein, A.; Jung, F. *Artif. Organs* **2012**, *36*, E28−E38.
(17) Roch, T.; Cui, J.; Kratz, K.; Lendlein, A.; Jung, F. *Clin. Hemorheol. Microcirc.* **2012**, *50*, 131−142.
(18) Braune, S.; Hönow, A.; Mrowietz, C.; Cui, J.; Kratz, K.; Hellwig, J.; Üzüm, C.; Klitzing, R. v.; Lendlein, A.; Jung, F. *Clin. Hemorheol. Microcirc.* **2011**, *49*, 375−390.
(19) Yoshikawa, H. Y.; Rossetti, F. F.; Kaufmann, S.; Kaindl, T.; Madsen, J.; Engel, U.; Lewis, A. L.; Armes, S. P.; Tanaka, M. *J. Am. Chem. Soc.* **2011**, *133*, 1367−1374.
(20) Hertz, H. *Z. Reine Angew. Math.* **1882**, *92*, 156−171.
(21) Sneddon, I. N. *Int. J. Eng. Sci.* **1965**, *3*, 47−57.
(22) Revilla, J.; A., E.; Carriere, P.; Pichot, C. *J. Colloid Interface Sci.* **1996**, *180*, 405−412.
(23) Sitti, M.; Cusick, B.; Aksak, B.; Nese, A.; Lee, H. I.; Dong, H. C.; Kowalewski, T.; Matyjaszewski, K. *ACS Appl. Mater. Interfaces* **2009**, *1*, 2277−2287.
(24) Lee, J. H.; Park, J. W.; Lee, H. B. *Biomaterials* **1991**, *12*, 443−448.
(25) Lee, J. H.; Jung, H. W.; Kang, I. K.; Lee, H. B. *Biomaterials* **1994**, *15*, 705−711.
(26) Bell, G. I. *Science* **1978**, *200*, 618−27.
(27) Bell, G. I.; Dembo, M.; Bongrand, P. *Biophys. J.* **1984**, *45*, 1051−1064.
(28) Bruinsma, R.; Behrisch, A.; Sackmann, E. *Phys. Rev. E* **2000**, *61*, 4253−4267.
(29) Bruinsma, R.; Sackmann, E. *C. R. Acad. Sci., Ser. IV: Phys. Astrophys.* **2001**, *2*, 803−815.
(30) Kawabe, M.; Tasaka, S.; Inagaki, N. *J. Appl. Polym. Sci.* **2000**, *78*, 1392−1401.
(31) Absolom, D. R.; Zingg, W.; Neumann, A. W. *J. Biomed. Mater. Res.* **1987**, *21*, 161−171.
(32) Sigal, G. B.; Mrksich, M.; Whitesides, G. M. *J. Am. Chem. Soc.* **1998**, *120*, 3464−3473.
(33) Arima, Y.; Iwata, H. *Biomaterials* **2007**, *28*, 3074−3082.